Exceedance frequency of the appearance of extreme internal waves in the World Ocean

Tatyana Talipova[1,2], Efim Pelinovsky[1,2], Oxana Kurkina[1], Ayrat Giniyatullin[1], Andrey Kurkin[1]

[1]Nizhny Novgorod State Technical University n.a. R.E. Alekseev, Nizhny Novgorod, 603950 Russia
[2]Institute of Applied Physics, Nizhny Novgorod, 603950 Russia

Correspondence to: Andrey Kurkin (aakurkin@gmail.com)

Abstract. Statistical estimates of internal waves ~~appearance~~ in different regions of the World Ocean are discussed. It is found that the observed exceedance probability of large-amplitude internal waves in most cases can be described by the Poisson law ~~curve~~, which is one of the typical distribution laws ~~curves~~ of extreme statistics. Detailed analysis of the statistical properties of internal waves in several regions of the World Ocean has been performed: tropical part of the Atlantic Ocean, ~~the~~ northwestern ~~North-West~~ shelf of Australia, the Mediterranean Sea near the Egyptian Coast, and the Yellow Sea.

Keywords: Internal waves, Exceedance frequency, Poisson statistics

1 Introduction

Internal waves are observed everywhere in the shelf zones of seas. The main source of their generation in the ocean is the semidiurnal tidal wave, which is initially barotropic and generates the baroclinic tidal wave by ~~the~~ scattering on the continental shelf. Periodical lunar tide M_2 generates internal waves with a period of 12.4 h. This process is well studied and presented in publications (Garret and Kunze, 2007; Morozov 1995; Vlasenko et al., 2005; Morozov 2018). Nevertheless the variability of the magnitude of the lunar tide and variations in the ~~daily~~ temperature and salinity of the sea water lead to random characteristics of the observed internal wave field, see, for example, book by Miropolsky (2001) and review paper by Helfrich and Melville (2006). Spectral and correlation methods of random internal wave field are widely applied in science. As a result, climatic spectra of internal waves have been determined. The well-known model of Garret and Munk (Garret and Munk, 1975), became the basis for the background spectra of internal waves in the World Ocean. This model determines the background of oceanic internal wave spectra, over which intense processes of internal wave generation occur leading to the appearance of large (up to extreme values of 500 m) amplitude internal waves (Alford et al., 2015). Data of the large-amplitude internal waves in various areas of the World Ocean are collected in numerous papers (Apel et al., 1985; Salusti et al., 1989; Holloway et al., 1999; Morozov 1995; Morozov 2018; Ramp et al., 2004; Sabinin and Serebryany, 2007; Shroyer et al., 2011; Xu and Yin, 2012; Kozlov et al., 2014; Xu et al, 2016). For example, extreme waves of high amplitudes in the Strait of Gibraltar and Kara Gates Strait were analyzed in (Morozov et al., 2002, 2003, 2008). Large-amplitude internal waves cause interest of researchers because of their dangerous impact on offshore platforms (Fraser, 1999; Song et al., 2011), their influence on safety of submarines and underwater vehicles (Osborn, 2010), they also cause phase fluctuations of acoustic signals over large distances (Warn-Varnas et al., 2003; Rutenko, 2010; Si et al., 2012;). The special warning systems are developed now in the regions of high risk of ~~a~~ pipe and platform damage by ~~the~~ intense internal waves (Stöber and Moum, 2011).

Internal waves in the ocean can be considered as a continuous random process, and their large amplitudes can be interpreted as outliers of a random process and can be described by the tails of the probability distribution functions. Consequently, the statistics of these processes is usually different from the Gaussian (normal) distribution. Non-Gaussian character of the observed internal wave field has been reported in many regions of the World Ocean (Miropol'sky, 2001; Wang and Gao, 2002; Pelinovsky, 1995). Seasonal and longitudinal statistical analysis of internal wave field has been reported recently in the South China Sea (Zheng et al, 2007). It is demonstrated ~~there~~ that the largest number of internal wave packets ~~here~~ is observed at a longitude of 116.5ºE (in the latitudinal band 20-22ºN). It has been reported that the most intense packets of internal waves in the South China Sea are generated in June. Special analysis of wave amplitude distribution in the tropical part of the West Atlantic, over the northwestern shelf of Australia, and in the eastern Mediterranean Sea has been performed in ~~papers~~ (Ivanov et al., 1993a,b; Pelinovsky et al., 1995). The authors show that the Poisson law is a good approximation for amplitude distributions of such waves. It is known [???] that the Poisson distribution is widely used in the extreme statistics and very often applied in the ocean engineering for describing storm waves (Pelinovsky and Kharif, 2016), tsunamis (Kaistrenko, 2014), rogue waves (Kharif et al., 2009); it is also used in geophysics for the description of climatic anomalies (Dischel, 2017), etc. However, the distribution law for temperature deviations in the tropical part of the East Atlantic (Mesopolygon-85) is more close to the Gaussian distribution (Morozov et al., 1998), which can be explained by lower energy of internal waves in this region.

In this paper we apply the methods of extreme statistics to large-amplitude internal waves and present a brief review. First, the theoretical approach is revised in Section 2. Then, the results of statistical processing of ~~the~~ internal wave records in various regions of the World Ocean are presented in Section 3. Conclusions are given in Section 4.

2 Extreme statistics methods for high amplitude internal waves

Let $\eta(t,|x,y,z)$ describe the vertical displacement of any isopycnal surface at fixed point, which, in the first approximation, can be considered as stationary random process. Usually, a few central moments

$$\mu_r = \int_{-\infty}^{\infty} (\eta - \overline{\eta})^r P(\eta) d\eta \qquad (r = 2, 3, 4) \tag{1}$$

are computed for the statistical analysis. Here $P(\eta)$ is the probability density function and $\overline{\eta}$ is the mean value $\overline{\eta} = \int_{-\infty}^{\infty} \eta P(\eta) d\eta$ (unperturbed position of isopycnal surface). The second moment $\mu_2 = \sigma^2$ determines the intensity of internal wave oscillations and σ is root mean square height of internal waves. The third and fourth moments determine skewness $Sk = \mu_3/\sigma^3$ and kurtosis $Ku = \mu_4/\sigma^4$, which are used to characterize the deviation of the distribution function from the Gaussian law (note that $Sk = 0$ and $Ku = 3$ for the Gaussian distribution). The sign of the skewness in our opinion can be explained by the specific shape in the Stokes internal wave, which follows from the weakly nonlinear theory of internal waves. Unlike nonlinear surface waves, which always have narrow and high crests and flat troughs, internal waves at different depths can have either narrow crests and flat troughs or vice-versa depending on the density stratification, modal structure, and distance to the bottom or surface. In the case of energetic internal waves of the first mode, the character of ~~the~~ asymmetry of wave profile with respect to the horizontal axis is determined by the coefficient of the quadratic nonlinear term in the Korteweg-de Vries equation, which is strongly variable in the World Ocean (Grimshaw et al., 2007; Kurkina et al., 2011, 2017a,b). Computations of the skewness and kurtosis as well as distribution function of nonlinear internal waves are ~~an~~ interesting problems, which are poorly studied.

Here we will use the direct method to evaluate the statistics of large-amplitude internal waves. We fix the reference vertical displacement and analyze the statistics of the exceedance of wave oscillations beyond this level (outliers of the random process). Let us briefly reproduce the well-known approach for calculating the exceedance frequency for continuous processes (Gumbel, 1958; Stuart, 2001) with application to ~~the~~ internal waves.

It is known from the vertical structure of internal waves that the largest amplitudes of the most energetic lowest-mode waves are found in the pycnocline. For definiteness, we chose the vertical displacement in the pycnocline and denote it $\eta(t)$ omitting coordinates of the pycnocline in this function. Both conditions for the outlier beyond level A in the interval Δt should be satisfied at once

$$\eta(t) < A \quad \text{and} \qquad \eta(t+\Delta t) > A. \tag{2}$$

Due to the smallness of Δt we can assume that $\eta(t+\Delta t) \approx \eta(t) + w(t)\Delta t$, where $w(t) = d\eta/dt > 0$ is the vertical velocity of water particles located within the isopycnal surface; we rewrite condition (2) as

$$A - w(t)\Delta t < \eta(t) < A. \tag{3}$$

The required probability of finding $\eta(t)$ in the interval (3) is

$$P(A - w\Delta t < \eta < A) = \int_0^{\infty} dW \int_{A-w\Delta t}^{A} f(\eta, W; t) d\eta, \tag{4}$$

where $f(\eta,w;\,t)$ is the two-dimensional probability density of vertical displacement $\eta(t)$ and ~~the~~ vertical velocity $w(t)$ at the same time moment and the same coordinates. Since Δt is small, we can use the mean-value theorem to calculate the inner integral in (4) and write:

$$P(\eta - w\Delta t < \eta < A) = \Delta t \int_0^\infty wf(A,w;t)dw \,. \quad (5)$$

Probability density function (in time) can be easily found from (5)

$$p(A;t) = \int_0^\infty wf(A,w;t)dw \,. \quad (6)$$

Similarly, the probability of crossing ~~the~~ level A from the top down (into the region of small value of isopycnal displacement) is

$$p'(A;t) = -\int_{-\infty}^0 wf(A,w;t)dw \,, \quad (7)$$

since this requires $w < 0$. This equation can be used to calculate the probability of large troughs (which can be as dangerous as large crests) in the vertical displacement. It is known that polarity of large internal waves in the ocean is usually negative; this correlates with the negative sign of the quadratic nonlinearity parameter in the weakly nonlinear theory based on the Korteweg-de Vries equation for the deepest parts of the World Ocean (Grimshaw et al, 2007).

Here, we calculate the average number of "positive" outliers (large crests) in the wave record. To do so we divide the total time interval into small subintervals Δt_j and introduce a random value N_j equal to 1 for an outlier and 0 outside the outlier. Then the total number of outliers is $N(A) = \sum N_j$ and its mean value is the ensemble average, the probability of this is equal to the probability of crossing ~~the~~ level (6). Moving on to the limit for $\Delta t_j \to 0$, we finally have

$$< N(A) >= \int_0^T \int_0^\infty wf(A,w;t)dwdt \,. \quad (8)$$

In the case of a stationary random process ~~the~~ formula (8) is simplified

$$< N(A) >= T \int_0^\infty wf(A,w)dw \,. \quad (9)$$

Thus, the average number of outliers is proportional to the time interval and decreases with the increase in the outlier level. The same approach can be used to compute the average number of "negative" outliers (the deepest troughs) in the internal wave field.

Only the average number of outliers was discussed above without considering their probabilistic distribution. A much more difficult problem is to calculate the latter. It should be noted that if outliers are rather rare (which is typical for very large-amplitude internal waves, $A \to \infty$), then their distribution can be regarded as the Poisson law. Then the probability that at least one outlier appears in the time interval t is

$$P = 1 - \exp(-\nu t), \tag{10}$$

where the mean frequency of outliers $\nu = \langle N \rangle / T$, is found from (9) as

$$\nu(A) = \int_0^\infty w f(A, w) dw. \tag{11}$$

The average frequency of outliers in the first approximation can be used as an estimate of the internal wave exceedance (cumulative) frequency with the amplitudes greater than the given value of A.

Detailed calculations of the outlier characteristics in the internal wave field require the knowledge of two-dimensional (vertical displacement and vertical velocity) distribution functions of isopycnal variation which are usually not measured. If the internal wave random field is assumed ~~to be~~ normal, the density of distribution function is described by the Gaussian law

$$f(\eta) = \frac{1}{\sqrt{2\pi}\delta} e^{-\frac{(\eta - \bar{\eta})^2}{2\delta^2}}, \tag{12}$$

where δ is the standard deviation (mean amplitude of ~~the~~ internal waves). The distribution function of the vertical displacement and the vertical velocity for the normal process do not correlate, hence, their two-dimensional probability density splits into a product of two Gaussian curves (12) with naturally have different mean-square deviations. Then, the average frequency of outliers can be written as

$$\nu(A) = \frac{\delta_w}{2\pi\delta_\eta} \exp\left(-\frac{A^2}{2\delta_\eta^2}\right), \tag{13}$$

where δ_w is the mean-square (standard deviation) value of the vertical velocity in the internal wave and δ_η is the mean-square value of the vertical isopycnal displacement. Thus, the internal wave exceedance frequency depends on the wave amplitude according to the Gaussian law, which rapidly decreases with increasing amplitude. We will demonstrate the Gaussian character of cumulative frequency for tropical zone of the East Atlantic Ocean.

One should remember that usually the statistical distributions of internal wave field in various regions of the World Ocean are different from the normal distribution as we have already pointed in the Introduction, see the book by Miropolsky (2001); hence, the result will be different from (13) depending on the particular form of the tails of the distribution function in large amplitude range. As it was shown in (Leadbetter et al., 1983), the intermediate asymptotic exceedance frequency for large outliers is described by the Poisson law

$$\nu = \nu_0 \exp\left(-\frac{A}{A_0}\right), \tag{14}$$

where ν_0 and A_0 are the parameters depending on the specific type of "tails" of the distribution function in the large amplitude range. This expression can be used to compute exceedance (cumulative) frequency of large outliers (positive or negative) in the internal wave field. Obviously, the predicted amplitude values are also random, and here one can speak only about its evaluation. Thus, to estimate the predicted amplitude A it is necessary to set the value of the exceedance frequency

$$\nu = 1/T, \tag{15}$$

where T is the prediction time (or the recording time). Expression (14) is used to calculate ~~the design~~ amplitude A of internal wave over prognostic time interval T

$$A_T = A_0 \ln(\nu_0 T). \tag{16}$$

Characteristic values of A_0 and ν_0 are different in various regions of the World Ocean and we shall discuss this in the next section.

3 Statistics of internal wave field

3.1. Probability density function in the Yellow Sea

Data analysis of measurements in the shallow water (Qingdao offshore area) of the Yellow Sea is reported in (Wang and Gao, 2002). The authors used a thermistor chain. The duration of records is 49 h 49 min with a sampling interval of 6.4 s. The water depth is 33 m. A thin unperturbed pycnocline is located in the interval from 10 m to 16 m with the maximum Brunt-Väisälä frequency N_{max} = 0.067 s^{-1}. Vertical displacements (double amplitudes!) of high-pass-filtered 25º - 17.5º (16 levels) isotherms are shown and their histograms are plotted. The maximum wave height did not exceed 5 m, nevertheless the process differs from the Gaussian process. It is found that the standard deviation is slowly increasing from 0.46 m to 0.56 m from the surface to the bottom. Skewness is negative for each isotherm and its maximum absolute value is 0.5 at a depth of 15 m; it decreases to 0.36 at the surface and to 0.06 close to the bottom. Kurtosis changes from 3.24 close to the bottom to 5.05 at a depth of 14 m and 4.12 near the surface. It is shown that the distribution of large internal wave amplitudes does not coincide with the Gaussian distribution.

We can explain the sign of the computed skewness applying the weakly nonlinear theory of internal waves based on the Korteweg-de Vries equation (Pelinovsky and Shurgalina, 2017). In this region of the Yellow Sea, the sign of quadratic nonlinear term in this equation is negative, because the water stratification (see ~~in~~ Wang and Gao, 2002) is practically approximated by a two-layer pycnocline located above the mid-depth (Djorjevich and Redekopp, 1978; Kakutani and Yamasaki, 1978). Nonlinear waves as solutions of the extended Korteweg-de Vries equation with negative quadratic nonlinearity have deeper troughs, for instance, internal solitons have negative polarity (Grimshaw et al., 2007). This leads to the negative values of ~~the~~ skewness.

3.2 Exceedance frequency of internal waves in the tropical zone of the West Atlantic

The exceedance frequency of internal waves is estimated using the data from the 39th cruise of the R/V “Akademik Vernadsky” in the Northwest Atlantic tropical zone near the mouth of the Amazon River, 2-15° N, 38-52° W (Ivanov et al., 1993b). Internal waves of moderate amplitudes from 2.5 to 10 m were observed in this region. The ship echo sounder was used to obtain long-term internal wave records. This device allowed the authors to study the fluctuations of the sound-scattering layer at depths up to 100 m. It is known that fluctuations of this layer can be caused by various processes, but in the range of periods up to 3 hour they are mainly related to internal waves. The wave period on the sonar records varies in a wide range from 3 min to 30 min. Since the measurements were made from the ship moving at a velocity of about V = 15 knots and as the maximum of internal wave speed is c = 3 knots ~~in order of magnitude~~, in the first approximation the internal wave pattern can be considered frozen. In this case, the “true” wave period increases in comparison to the observed one with a ratio of V/c = 5. The amplitude of sound-scattering layer fluctuations was everywhere associated with internal wave amplitude in the pycnocline. The total record duration was about 218 hours. Wave height (defined as the fluctuation swing between adjacent extreme values) and fluctuation duration of the records were considered the main characteristics. The main results of daily echogram processing are presented in ~~the paper~~ (Ivanov et al., 1993b). These data are used to estimate the exceedance (cumulative) frequency. They agree well with the regression line

$$\nu = 9.2\exp(-0.3H) , \qquad (17)$$

where H is the wave height measured in meters, and the dimension of ν is [hr^{-1}], except for the heights greater than 25 m, where the total number of wave observations does not exceed six. Expression (17) is used to estimate the predicted wave height versus predicted time function

$$H = 18 + 3.3\ln T . \qquad (18)$$

Predicted values of internal wave heights versus time are summarized in Table 1.

During the time of measurements in the region, the “true” internal wave recording time (considering the ship motion) was about 45 days. According to the prediction for this period, a wave with a height of more than 31 m should be observed once, with a height of more than 27 m – twice, and more than 23 m – three times. In fact, the level of 31 m was exceeded three times, and the level of 27-28 m was exceeded six times, which indicates that a good agreement exists between the measurements and the predictive models.

3.3 Temperature fluctuations caused by internal waves at Mesopolygon-85 in the Atlantic Ocean

It is expected that the wave process in the open ocean are described by the normal law, which makes it possible to use the theory of normal random process and estimate the limits of its applicability for internal waves. In this paper, the exceedance frequency analysis is undertaken for internal wave records obtained from a cluster of moorings in the East Atlantic Ocean in 1985 (the Mesopolygon-85 experiment; the detailed description of the experiment is given in Kort, 1988). Seventy-six moorings with current and temperature meters were deployed in the study area called Mesopolygon- 85 in the eastern part of the Atlantic Ocean with the objective of studying mesoscale variability of hydrophysical processes. The study site was located between the Canary Basin and the Cabo Verde Basin (19-21°N and 36-38°E). The moorings operated approximately for two months from April to May. The instruments were set at four levels, but the most representative measurements were gathered at a level of 200 m. The total size of the study site was approximately 80 by 80 miles. The sampling interval was 15 min. In the Mesopolygon area, the bottom is covered with hills from 500 to 1000 m high over the sea floor. Such hills are located every 10 or 20 miles. They form a corrugated bottom topography over which the horizontal streamlines of barotropic currents are deformed. Thus, the internal tide is generated immediately in this area over the deep-sea bottom topography. It should be mentioned that 49 buoy records are available in the region, and it is a unique possibility to estimate the horizontal variability of the internal wave amplitude distribution function.

Records of temperature variations (centigrade) at various points of the study site were used to calculate the average frequency of outliers (temperature variation exceeding the fixed value ΔT). All processed records are very well described by the Gaussian distribution

$$\nu = (0.79 \pm 0.17)\exp\left(-(10.61 \pm 4.5)(\Delta T)^2\right), \qquad (19)$$

where the parameters vary from station to station. The dimension of ν is hr^{-1} and ΔT is in centigrade. It should be noted that the deviation in ν_0 are from 21% to 42% in the exponent, over a study site of 48000 km^2 in the tropical part of the East Atlantic. More details of the experiment data are given in (Morozov et al., 1998).

3.4 Internal wave heights in the Mediterranean Sea

Let us discuss internal wave statistics in the seas of low tide, where one can expect the universe statistical characteristics over a short period of time without correlation to the phases of the moon. The mechanisms of internal wave generation here may be such as storms and upwelling as well as the effect of river discharge. We analyze internal wave observations in one of the Mediterranean regions (the Levant Sea) ~~obtained~~ during cruise 27 of the RV "Professor Kolesnikov" (July-August 1991). These old data briefly presented in (Ivanov et al. 1993a) are now revised. During the period from 27 to 29 July, 1991 a special experiment to record internal waves was performed in the study site near the Egyptian shelf. A distributed temperature sensor 25 m long (MHI 4106) has been towed in the thermocline along the tacks located as a star. The temperature data were later recalculated into the vertical isopycnal displacements. The basin depth in the study site varies from 200 to 1100 m. The vertical profile of the Brunt-Väisälä frequency in the pycnocline at a depth of about 25 m is characterized by a frequency of 17 cycle/hour. Below the pycnocline, the mean value of the Brunt-Väisälä frequency was about 4 cycle/hour. The wave height distribution function has been calculated from these data. The vessel speed was approximately V = 5 knots, which significantly exceeds the internal wave propagation speed in this region (c = 2 knots). Therefore, in the first approximation, the internal wave field can be considered ~~as~~ frozen. This means that the “true” time recording can be increased by V/c = 2.5 times. The applicability of the Gaussian (red) and Poisson (blue) laws for the exceedance (cumulative) frequency, as one can see from Fig. 1, is well applicable to the observed data: they are approximated by the formulas

$$\nu = 4\exp(-1.9A), \text{ (a)} \qquad \nu = 2\exp(-A^2) \text{ (b)} \tag{20}$$

where A is a wave amplitude measured in meters, and ν is in hr^{-1}. Distribution ~~The obtained distribution~~ (20) can be used for the prediction of relatively large amplitude waves. The predicted values of internal wave amplitudes calculated using formula (20a) that can occur in the Mediterranean Sea near the Egyptian shelf over different time periods, are summarized in Table 2.

It should be noted that the observed internal waves in this region have much smaller amplitudes than over the ridges, for example, the Mascarene Ridge (Morozov et al., 1996) or in the Luzon Strait where 100-meter waves are recorded (Ramp et al., 2004). This fact is well known in the seas with low tides and is reflected in the large value of the return period for internal wave of 5 m amplitude in this part of the Mediterranean Sea (WHAT IS RETURN PERIOD?). Hence, the observed height distribution is between the Gaussian statistics (for weak-amplitude waves) and Poisson statistics (for large-amplitude waves).

3.5 Exceedance frequency in the current velocity from the mooring data ~~of buoy stations~~ (~~the~~ north-western shelf of Australia)

Relatively long internal wave records were obtained from moorings on the northeastern shelf of Australia (Pelinovsky et al., 1995). The water depth is approximately 123 m. We shall analyze the velocities in the internal wave range, recorded at 3 m above the ocean bottom. The time sampling was 2 min, and the duration of measurements was 10 days. Only the velocity component, which contains the strongest wave fluctuations, was analyzed in the direction transverse to the isobaths (45^0 northeast). The time series were processed by a high-frequency filter to remove the tidal component. Each record was divided into equal intervals of 4000 minutes. The analysis of time series processing results is reported by Pelinovsky et al. (1995). The calculated values of exceedance frequency for different amplitudes are approximated by ~~the~~ expression

$$\nu = 1.33\exp(-0.071U), \tag{21}$$

where the dimension of ν is hr^{-1} and the dimension of the amplitude of horizontal velocity variation U is cm/sec.

The regression formulae presented above can be used to calculate the exceedance probability of large-amplitude internal waves as function of the amplitude of velocity caused by internal waves and time duration. The results of calculation for the North West Shelf of Australia are shown in Fig. 2.

4 Conclusions

We have considered statistical characteristics of the internal wave field in several zones of the World Ocean: the tropical part of the West Atlantic Ocean near the Amazonian mouth, a part of the East Atlantic, the western part of the Mediterranean Sea, the northwestern shelf of Australia, and the Yellow Sea shelf (Fig. 3).

It is difficult to compare directly the results of exceedance frequency calculations in various regions of the World Ocean. (THE DIFFICULTIES IN COMPARISON IS NOT A CONCLUSION OF THIS WORK; HENCE THE ENTIRE PARAGRAPH SHOULD BE MODED ABOVE TO THE END OF DESCRIPTIONS). The main difficulty of the comparison is that different characteristics were measured. In particular, in the tropical zone of the Atlantic, the vertical displacement of the sound-scattering layers was measured, in the Mediterranean Sea it was the amplitude of displacement of the thermocline, while on the Australian shelf the records of flow velocity fluctuations were analyzed, and at the Mesopolygon-85 it was the temperature fluctuations at a given level. The internal mode structures were never analyzed using these measurements, and ~~we cannot confirm that~~ the observations were not performed using similar methods. ~~in the mode maximum~~. ~~So, we may predict the internal wave amplitude only at the level of measurements~~. ~~Also for three analyzed areas~~ The Poisson law is valid for internal wave amplitude distribution in the three study sites, but in Mesopolygon - 85 we get the Gaussian distribution which is more appropriate for very small amplitudes. However, the amplitudes of internal waves in the eastern Mediterranean Sea do not exceed 2 m but the amplitude distribution function is closer to the Poisson law. It seems that the analysis presented here is the subject for the further research. (IT IS NOT A CONCLUSION OF THE RESEARCH) Meanwhile, the value of ν_0 has universal character and should not depend on the measured characteristics of internal waves. In the Australian shelf ν_0 = 1.3 hr^{-1}, in the tropical zone of the Atlantic ν_0 = 9.2 hr^{-1}, in the Mesopolygon-85 ν_0 = 0.8 hr^{-1} and in the Mediterranean (Levant Sea) ν_0 = 4 hr^{-1}. The scatter of these values is very high. Each value is characteristic of the specific ocean region. We can attribute this difference to the intensity of internal wave generation in various regions of the ocean. It is known that tropical South Atlantic is a region of large - amplitude internal waves due to the strong generation of internal tides by the interaction between the barotropic tide and bottom topography (Morozov, 1995). Low amplitude ~~but often generated~~ internal waves were observed near the Nile River mouth. THE JUMP BETWEEN THESE TWO SENTENCES SHOULD BE MADE SMOOTHER Internal waves are generated mainly by the tide propagating across the Australian shelf. In the northwestern Australian shelf, internal waves are generated mainly be the barotropic tide interacting with the slope. We may assume on the basis of the value ν_0 = 0.8 hr^{-1} that internal waves of high amplitudes are not often recorded in the region of Mesopolygon-85, but internal waves of moderate amplitude are always generated.

Currently, the numerical methods to predict internal wave field characteristics in different regions of the World Ocean are widely applied. Calculations demonstrate that their characteristics are very sensitive to the density stratification of the ocean. The influence of variation of water stratification on the internal wave dynamics can be illustrated by the seasonal maps of kinematic parameters of internal waves (Kurkina et al., 2001, 2017a,b). Statistical estimates of internal waves existing in various regions under different background conditions using numerical models have been calculated. Such computations have been done already within the Euler equations for stratified water in the Barents Sea (Kurkina and Talipova, 2011; Talipova et al., 2014) and in the Sea of Okhotsk (Kurkina et al., 2017b) etc. THE STATEMENTS IN THIS PARAGRAPH ARE NOT CONCLUSIONS OF THE RESEARCH AND DO NOT CARRY USEFUL INFORMATION.

Data availability. The data used by this study are extracted from the GDEM database.

Competing interests. The authors declare that they have no conflict of interest.

Acknowledgements. This study was initiated in the framework of the state task programme in the sphere of scientific activity of the Ministry of Education and Science of the Russian Federation (projects No. 5.4568.2017/6.7 and No. 5.1246.2017/4.6) and financially supported by this programme, grants of the President of the Russian Federation (NSh-2685.2018.5 and MK-1124.2018.5) and Russian Foundation for Basic Research (grant No. 16-05-00049).

Authors thank Eugene Morozov and Yury Stepanyants for useful critical comments

References CHECK THE REFERECNCES AND CHANGE росмотрите литературу на предмет заглавных букв в названиях статей, чтобы было однотипно

Alford, M.H., Peacock, T., MacKinnon, J.A., Nash, J.D., Buijsman, M.C., Centurioni, L.R., Chao, S.Y., Chang, M.H., Farmer, D.M., Fringer, O.B., Fu, K.H., Gallacher, P.C., Graber, H.C., Helfrich, K.R., Jachec, S.M., Jackson, C.R., Klymak, J.M., Ko, D.S., Jan, S., Johnston, T.M.S., Legg, S., Lee, I.H., Lien, R.C., Mercier, M.J., Moum, J.N., Musgrave, R., Park, J.H., Pickering, A.I., Pinkel, R., Rainville, L., Ramp, S.R., Rudnick, D.L., Sarkar, S., Scotti, A., Simmons, H.L., St Laurent, L.C., Venayagamoorthy, S.K., Wang, Y.H., Wang, J., Yang, Y.J., Paluszkiewicz, T., and Tang, T.Y.: The formation and fate of internal waves in the South China Sea, Nature, 521, P. 65-69, 2015,

Apel, J.R., Holbrock, J.R., Kiu, A.K., and Tsai, J.J.: The Sulu Sea internal soliton experiment, J. Phys. Oceanogr., 15, 1625-1651, 1985.

Dischel, R.S., (Ed): Climate Risk and the Weather Market, Incisive Risk Information (IP) Limited, 2017.

Djordjevic, V.D., and Redekopp, L.G.: The fission and desintegration of internal solitary waves moving over two-dimensional topography, J. Phys. Oceanogr., 8, 1016-1024, 1978.

Fraser, N.: Surfing an oil rig, Energy Rev., 20(4), 1999.

Garrett C, Kunze E (2007) Internal tide generation in the deep ocean. Annual Rev. Fluid Mech. 39: 57–87

Garrett, C.G.R., and Munk, W.H.: Space-time scales of internal waves: a progress report, Jour. Geophys. Res., 10(3), 291-297, 1975.

Grimshaw, R., Pelinovsky, E., and Talipova, T.: Modeling internal solitary waves in the coastal ocean, Survey in Geophysics, 28(2), 273-298, 2007.

Gumbel, E.J.: Statistics of Extremes, Columbia Univ. Press, New York, 384, 1958.

Helfrich, K.R., and Melville, W.K.: Long Nonlinear Internal Waves, Annu. Rev. Fluid Mech., 38, 395-425, 2006.

Holloway, P., Pelinovsky, E., and Talipova, T.: A generalised Korteweg-de Vries model of internal tide transformation in the coastal zone, J. Geophys. Res., 104, 18333-18350, 1999.

Ivanov, V.A., Pelinovsky, E.N., and Talipova, T.G.: Recurrence Frequency of Internal Wave Amplitudes in the Mediterranean, Oceanology, 33(2), 180-184, 1993a.

Ivanov, V.A., Pelinovsky, E.N., and Talipova, T.G. The long-time prediction of intense internal wave heights in the tropical region of Atlantic, J. Phys. Oceanography, 23(9), 2136-2142, 1993b.

Kaistrenko, V.: Tsunami, Recurrence Function: Structure, Methods of Creation, and Application for Tsunami Hazard Estimates, Pure Appl. Geophys.,171, 3527-3538, 2014.

Kakutani, T., and Yamasaki, N.: Solitary waves on a two-layer fluid, J. Phys. Soc. Japan, 45, 674-679, 1978.

Kharif, Ch., Pelinovsky, E., and Slunyaev, A., Rogue Waves in the Ocean, Springer, 216, 2009.

Kozlov, I., Romanenkov, D., Zimin, A., and Chapron, B.: SAR observing large-scale nonlinear internal waves in the White Sea, Remote Sensing of Environment, 147, 99-107, 2014.

Kurkina, O., and Talipova, T.: Huge internal waves in the vicinity of Spitsbergen Island (Barents Sea), Natural Hazards Earth System Sciences, 11, 981–986. 2011.

Kurkina, O., Talipova, T., Pelinovsky, E., and Soomere, T.: Mapping the internal wave field in the Baltic Sea in the context of sediment transport in shallow water, J Coastal Research, SI, 64, 2042-2047, 2011.

Kurkina, O., Rouvinskaya, E., Talipova, T. and Soomere, T.: Propagation regimes and populations of internal waves in the Mediterranean Sea basin, Estuarine, Coastal and Shelf Science, 185, 44-54, 2017a.

Kurkina, O.,, Talipova, T. , Soomere, T., Kurkin, A., and Rybin, A.: The impact of seasonal changes in stratification on the dynamics of internal waves in the Sea of Okhotsk, Estonian Journal of Earth Sciences, 66(4), 238-255, 2017b.

Kort, V.G. (Ed.): Hydrophysical studies on the program "Mesopolygon", M., Nauka, 1988.

Leadbetter, M.R., Lindgren, G., and Rootzen, H.: Extremes and Related Properties of Random Sequences and Processes, Springer, 1983.

Miropolsky, Yu. Z.: Dynamics of internal gravity waves in the ocean, Kluwer Academic Publishers, Boston, 421, 2001.

Miropolsky Y.Z. (2001) Dynamics of Internal Gravity Waves in the Ocean. Shishkina O. (ed). Springer

Morozov E.G. Semidiurnal internal wave global field, Deep Sea Research, vol. 42, No 1, 1995, 135-148

Morozov E.G. Oceanic Internal Tides, Observations, analysis, and modeling. A global view. Springer 2018.

Morozov E.G., Vlasenko V.I. Extreme tidal internal waves near the Mascarene Ridge. J. Marine Systems, V.9 (3-4), p. 203-210, 1996

Morozov, E., Pelinovsky, E., and Talipova, T.: Exceedance Frequency for Internal Waves during the Mesopolygon-85 Experiment in the Atlantic, Oceanology, 38(4), 470-475, 1998.

Morozov E.G., Trulsen K., Velarde M.G., and Vlasenko V.I., Internal tides in the Strait of Gibraltar, J. Physical Oceanography, vol. 32, 3193-3206, 2002.

Morozov E.G., Parrilla-Barrera G., Velarde M.G., Scherbinin A.D., The Straits of Gibraltar and Kara Gates: A Comparison of Internal Tides, Oceanologica Acta, Vol. 26 (3), 231-241, 2003.

Morozov E.G., Paka V.T., Bakhanov V.V., Strong internal tides in the Kara Gates Strait, Geophysical Research Letters, p. L16603, 2008.

Osborne, A.: Nonlinear Ocean Waves and the Inverse Scattering Transform, Academic Press, 944, 2010.

Pelinovsky, E., Holloway, T., and Talipova, T.: A statistical analysis of extreme events in current variations due to internal waves from the Australian North West Shelf, J. Geophys. Res., 100(C12), 24831-24839, 1995.

Pelinovsky, E., and Kharif, C. (Eds): Extreme Ocean Waves. 2d Edition, Springer, 236, 2016.

Pelinovsky, E., and Shurgalina, E.: KDV soliton gas: interactions and turbulence. Book: Challenges in Complexity: Dynamics, Patterns, Cognition (Eds: I. Aronson, N. Rulkov, A. Pikovsky, L. Tsimring), Series: Nonlinear Systems and Complexity, Springer, 20, 295-306, 2017.

Ramp, S.R., Tang, T.Y., Duda, T.F., Lynch, J.F., Liu, A.K., Chiu, C.S., Bahr, F.L., Kim, H.R., and Yang, Y.J.: Internal solitons in the northeastern South China Sea - Part I: Sources and deep water propagation, IEEE J. Ocean. Eng., 29(4), 1157-1181, 2004.

Rutenko, A.N.: The influence of internal waves on losses during sound propagation on a shelf, Acoustical Physics, 56, 703-713. 2010.

Sabinin, K.D., and Serebryany, A.N.: “Hot Spots” in the Field of Internal Waves in the Ocean, Acoustical Physics, 53(3), 357-380, 2007.

Salusti, F., Lascaratos, A., and Nittis, K.: Changes of polarity in marine internal waves: Field evidence in eastern Mediterranean Sea, Ocean Modelling, 82, 10-11, 1989.

Shroyer, E.L., Moum, J.N., and Nash, J.D.: Nonlinear internal waves over New Jersey’s continental shelf, J. Geoph. Res., 116, C03022, 2011.

Si, Z., Zhang, Y., and Fan, Z.: A numerical simulation of shear forces and torques exerted by large-amplitude internal solitary waves on a rigid pile in South China Sea, Appl. Ocean Res., 37, 127-132, 2012.

Song, Z.J., Teng, B., Gou, Y., Lu, L., Shi, Z.M., Xiao,Y., and Qu, Y.: Comparisons of internal solitary wave and surface wave actions on marine structures and their responses, Applied Ocean Research, 33, 120-129, 2011.

Stöber, U., and Moum J.N.: On the potential for automated realtime detection of nonlinear internal waves from seafloor pressure measurements, Appl. Ocean Res., 33, 275-285, 2011.

Stuart, C.: An Introduction to Statistical Modeling of Extreme Values, Springer, 242, 2001.

Talipova, T.G., Kurkina, O.E., Terletska, E.V., Kurkin, A.A., and Rouvinskaya, E.A.: Modeling of internal wave field in the coastal zone of the Barents Sea, Ecological Systems and Devices, 3, 26-38, 2014.[in Russian]

Xu, J., Chen, Zh. , Xie, J.,. and Cai, Sh.: On generation and evolution of seaward propagating internal solitary waves in the north western South China Sea, Commun Nonlinear Sci Numer Simulat, 32, 122-136, 2016.

Xu, Zh., and Yin, B.: Variability of Internal Solitary Waves in the Northwest South China Sea, Oceanography, Prof. Marco Marcelli (Ed.), ISBN: 978-953-51-0301-1, InTech., 2012.

Vlasenko, V., Stashchuk, N., and Hutter, K.: Baroclinic Tides: Theoretical Modeling and Observational Evidence, Cambridge University Press, 351, 2005.

Wang, T., and Gao, T.: Statistical properties of high-frequency internal waves in Qingdao offshore area of the Yellow Sea, Chinese Journal of Oceanology and Limnology, 20(1), 16-21, 2002.

Warn-Varnas, A. C., Chin-Bing, S.A., King, D. B., Hallock, Z., and Hawkins, J.A. Ocean-acoustic solitary wave studies and predictions", Surveys in Geophysics, 24, 39-79, 2003.

Zheng, Q., Susanto, R.D., Ho, Ch.-R., Song, Y.T., and Xu, Q.: Statistical and dynamical analyses of generation mechanisms of solitary internal waves in the northern South China Sea, J. Geophys. Res., 112, C03021, 2007.

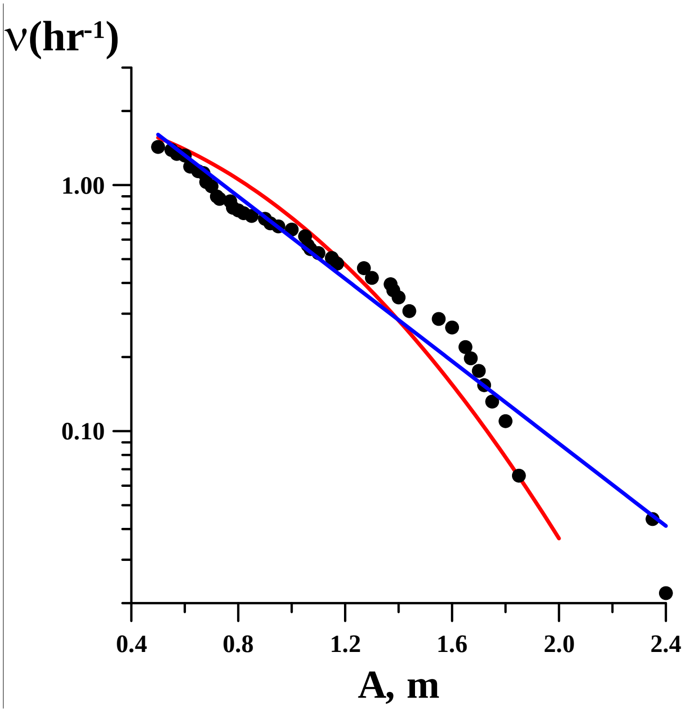

Figure 1: The exceedance frequency of internal wave amplitudes in the eastern part of the Mediterranean Sea.

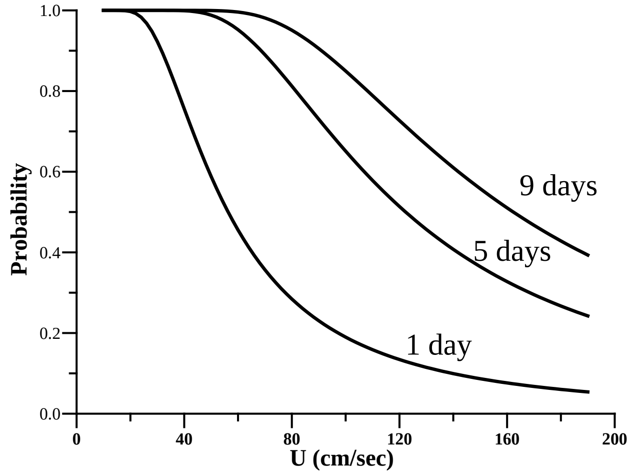

Figure 2: Probability of occurrence of internal waves at the North West Australian shelf.

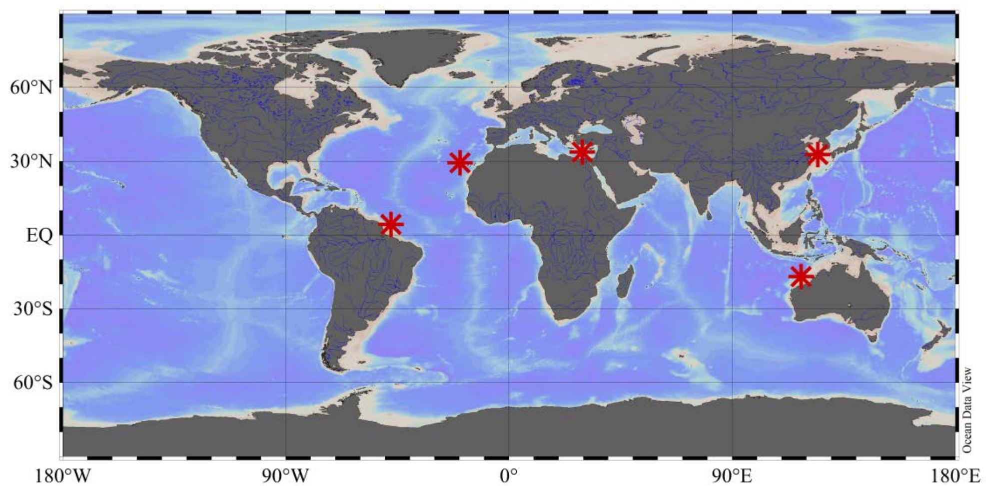

Figure 3: Areas, where we consider statistical characteristics of internal waves.

Table 1: Wave height prediction for the Atlantic tropical zone.

time	1 day	10 days	1 month	3 months	6 month	1 year
***H*(m)**	18	26	29	33	35	38

Table 2: Predicted internal wave heights in the Mediterranean Sea.

Time period	1 day	1 week	1 month	3 months
***A*(m)**	2.6	3.6	4.5	5.1